2. LITERATURE REVIEW

2.1 Intelligent Packaging

Intelligent packaging is defined as a packaging system that monitors the condition of packaged food to give information about the quality of the packaged food during transport and storage (Ahvenainen R., 2003).

Intelligent packaging is defined as a packaging system that is capable of carrying out intelligent functions (such as detecting, sensing, recording, tracing, communicating, and applying scientific logic) to facilitate decision making to extend shelf life, enhance safety, improve quality, provide information, and warn about possible problems (Yam L. K. *et al.*, 2005).

Many intelligent packaging concepts which are used to determine the quality of packaged food involve external indicator i.e. indicators which are attached outside the package (time temperature indicator) and internal indicators which were placed inside the package, either to the head-space of the package or attached into the lid (oxygen indicators, carbon dioxide indicators, microbial growth indicators and pathogen indicators).

Table 2.1 Examples of external and internal indicators and their working principle or reacting compounds to be used in intelligent packaging for quality control of packed food (Ahvenainen R. *et al.*, 2003)

Indicator	Principle/reagents	Give information about	Application
Time-temperature indicators (external)	Mechanical Chemical Enzymatic	Storage condition	Foods stored under chilled and frozen conditions
Oxygen indicators (internal)	Redox dyes pH dyes Enzymes	Storage condition Package leak	Food stored in packages with reduced oxygen concentration
Carbon dioxide indicator (internal)	Chemical	Storage condition Package leak	Modified/controlled atmosphere food packaging

Indicator	Principle/reagents	Give information about	Application
Microbial growth indicators (internal/external) i.e. freshness indicators	pH dyes All dyes reacting with certain metabolites (volatiles or non-volatiles)	Microbial quality of food (i.e. spoilage)	Perishable foods such as meat, fish and poultry
Pathogen indicators (internal)	Various chemical, immunochemical methods reacting with toxins	Specific pathogenic bacteria such as Escherichia coli O157	Perishable foods such as meat, fish and poultry

2.2 Freshness Indicator

Freshness indicators are used to indicate the product quality information resulting from microbial growth or chemical changes within a food product during storage and transportation. One of concepts for freshness indicator are presented based on indicators sensitive to pH change, which change color in the presence of volatile compounds produced during spoilage. The indicator exhibits the irreversible change in visual appearance due to microbial growth during food deterioration inducing pH change. Volatile nitrogen compound, carbon dioxide, hydrogen sulphide and organic acid are proposed to be suitable target molecules for pH-sensitive indicators.

For example, Hong *et al.* (2000) studied the use of color indicators as a packaging system for evaluating kimchi fermentation. The color indicating films consisted of polypropylene (PP) resin, calcium hydroxide as a CO_2 absorbent and bromocresol purple (BP) or methyl red (MR) as a chemical dye. Kimchi fermentation was assessed for titratable acidity (TA) and color changes of the indicators were measured and expressed as Hunter values as well as total color difference (TCD). From the color data, TCD values of bromocresol purple (BP) type indicator ranged 27±33 and were much more than those of methyl red (MR) type. In the case of BP, Hunter L and b values increased gradually with storage time while Hunter a value decreased slowly and then remained constant. However, Hunter L and b values of the

indicator containing MR decreased exponentially while Hunter a value increased remarkably and remained constant. The result means that color of the BP type indicator turned from initially blue to finally light green, and that of the MR type turned from light orange to red. The rate of color changes was different depending on temperature but with the same pattern. Moreover, TCD of each indicator closely correlated with TA, as little influenced by temperature. The TA values give a nearly straight line against the TCD values of the BP type indicator, whereas they formed a concave curve over those of the MR type. Present result suggests that the BP type indicator can be used successfully as a full time-fermentation indicator for kimchi products. However, the MR type may be applied only as a ripeness/unripeness indicator to packaged kimchi because its color change rate nearly reaches to zero at the TA values more than 0.7 mg/dl.

Tassanawat *et al.* (2007) prepared pH-sensitive modified clay and polypropylene nanocomposites for smart packaging to represent the degree of deterioration of fresh milk. Milk deterioration was assessed for titratable acidity (TA) and color change of the bromothymol blue (BMB) as an indicator was measured by total color difference (TCD) value. The result of TA and TCD values suggested that BMB can be used as fresh milk deterioration indicator. The nanoclay composites incorporating pH indicator were melt compounding through a twin screw extruder using surlyn® as a reactive compatibilizer. Subsequently, the nanoclay composites were fabricated into the sample sheet for pH-sensitive test.

Nopwinyuwong *et al.* (2010) prepared a colorimetric mixed pH dye-based indicator for the development of intelligent packaging as a chemical barcode for real-time monitoring of intermediate-moisture dessert spoilage. The on-package indicator contains mixed pH-sensitive dyes, bromothymol blue and methyl red, that respond through visible color change to CO_2 as a spoilage metabolite. The result of the change in CO_2 level monitored by the indicator label in golden drop at 25 and 10°C showed that a clear spectrum from bright light green to orange-red corresponded with exposed CO_2 during storage time. The minimal spoilage level of golden drop occurred on days 6 and 28 during storage at 25 and 10°C respectively as shown in Figure 2.1.

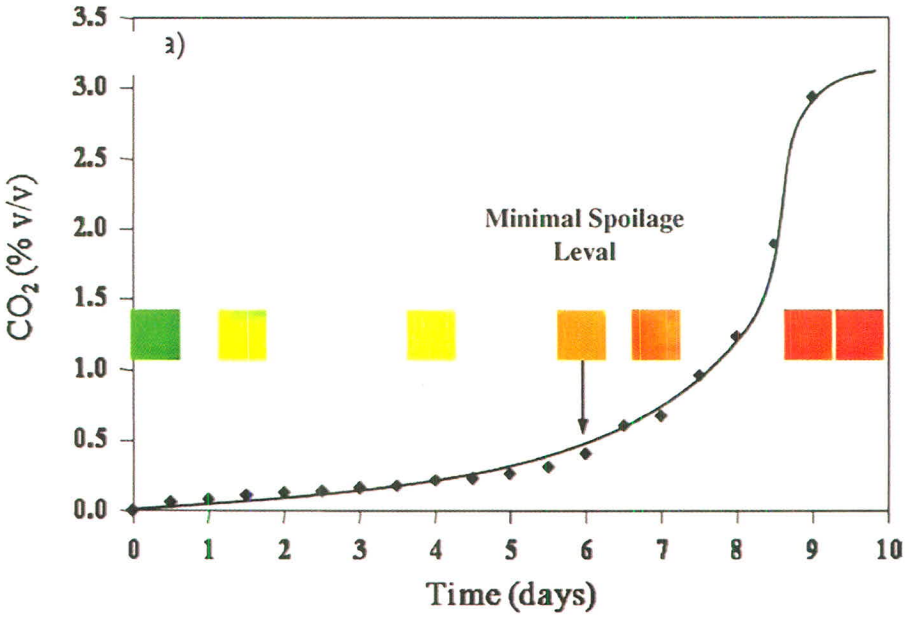

Figure 2.1 Change in CO_2 level in golden drop at 25°C with indicator level which showed color change with time.

2.3 Climacteric Fruit Freshness

Generally, fruits can be classified as climacteric and non-climacteric. Climacteric is defined as a period in the ontogeny of certain fruits, during which a series of biochemical changes is initiated by the autocatalytic production of ethylene, marking the change from growth to senescence and involving an increase in respiration and leading to ripening. The ripening of climacteric fruit associates with increasing in respiration and ethylene production. The respiration rate will rise up to the climacteric peak and then decline. The majority of fruits that show the climacteric pattern are the apple, apricot, avocado, banana, cherimoya, cantaloupe melon, mango, papaya, passion fruit, pawpaw, peach, pear, plum and tomato.

The climacteric patterns are different in each fruit. For example, the respiration rise of apple and tomato occurs both in fruit detached from and attached to the vine while the avocado only shows a climacteric rise in respiration after detachment from the tree. In many types of tropical and sub-tropical fruits, the rise in

respiration is rapid and the stage of eating ripeness corresponds closely with the climacteric peak in fruits such as avocado, banana, cherimoya and mango. This differs from the apple and tomato which ripening is not complete until after the climacteric peak. Thus in tropical fruits, the various changes involve in the climacteric and ripening show a more complete overlap in time. Moreover, the patterns of respiration and ripening behavior vary among the varieties, the climacteric conditions and the local places.

Respiration can be described as the oxidative breakdown of the more complex materials normally present in cell, such as starch, sugars and organic acids, into simple molecules, such as carbon dioxide and water, with the concurrent production of energy and other molecules that can be used by the cell for synthesis reaction.

The respiration process can be divided into two types, aerobic respiration and anaerobic respiration. Aerobic respiration is a complicated process that involves the enzymatic reaction taking place through the metabolic pathways of glycolysis, the tricarboxylic acid (TCA) cycle, and the association electron transport system. However, the overall reaction describing the respiration process may be simply expressed as

$$C_6H_{12}O_6 + 6O_2 \longrightarrow 6CO_2 + 6H_2O + \text{energy} \qquad (1)$$

Anaerobic respiration, which is sometimes called fermentation, involves the incomplete oxidation of compounds in the absence of O_2 and the accumulation of ethanol, acetaldehyde and CO_2. The respiratory quotient (RQ) is the ratio of CO_2 produced to O_2 consumed during respiration. This is used to identify the type of respiration process. Values of RQ range from 0.7-1.3 for aerobic respiration, depending on the substance being oxidized for carbohydrates, RQ = 1; for lipids RQ < 1; for organic acid RQ> 1. Respiration rate is a good indicator of the likely storage life of horticultural products. The storage life of produces is proportional to the respiration rate a horticultural commodity with a low respiration rate has a longer storage life. For example: apples, citrus fruit, grapes and kiwi fruit. By contrast, high

respiration rate commodities such as strawberry, blackberry, raspberry, avocado and mango have a much shorter storage life (Jirapattarasakul, 2002).

Gane *et al.* (1936) studied the respiration of banana. The respiration of bananas has been measured with fruit of various stages of ripeness under a variety of experimental conditions. First, the respiratory activity in the preclimacteric phase of green and unripe bananas at different temperature was studied. The mean values of the rate of respiration as a function of temperature are shown in Table 2.2. During this time the rate of respiration remains almost steady except at 31°C. The rate of production of carbon dioxide in the preclimacteric phase decreased with time and at this temperature one might expect the onset of a time factor.

Table 2.2 Rate of respiration of green bananas at different temperatures

Temperature (°C)	0	5	12.5	15	20	31
Rate of Respiration (mg/kg/hr)	7.1	10.0	18.5	23.6	35.8	61

Then, the ripening process at different temperature was studied. The characteristic form of the curve of respiratory activity during the ripening process at different temperatures was shown in Figure 2.2. Although the preclimacteric value is practically constant at any temperature, the peak value is not so constant. The effect of temperature on the ripening process as distinct from the time required for ripening to commence can be illustrated by comparing the time taken for the respiration to rise from the pre-ripening phase to the peak value and the times were shown in Table 2.3. Moreover, it was found that the change of color from green to yellow begins to be visible at the peak of respiratory activity, so that fruit may appear to be green and unripe and yet be well advanced on the climacteric. Banana showed the downward drift does not continue after the peak and there was a period when the rate was almost steady. This was followed by a period when it roses again. These changes in the rate of output of carbon dioxide coincided with the changes in the eating quality of the fruit. Just before the respiration has become steady, the fruit has developed its

full yellow color and the eating quality is at its optimum. From this stage onwards the flavor increased in intensity until finally, at the fully ripe stage, it was too pronounced to be palatable. The relation of these stages to the course of respiration at 15° C was shown in Figure 2.4 where *FYC* refers to the full-yellow-color stage and *FR* to the fully ripe stage.

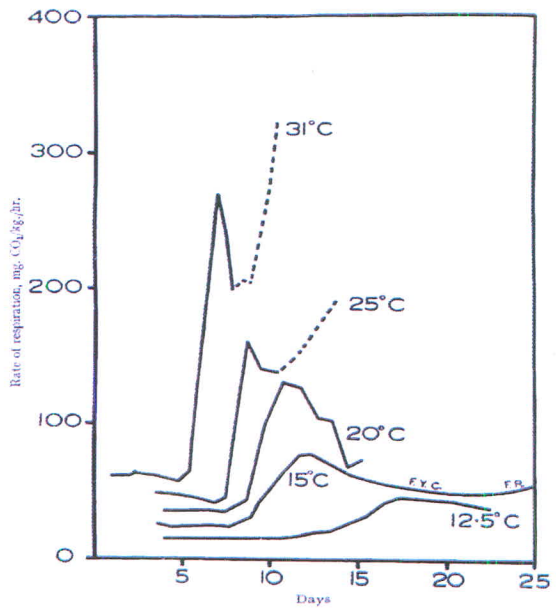

Figure 2.2 Rate of production of carbon dioxide by bananas (initially unripe) at different temperatures.

Table 2.3 The times of respiration rise from pre-ripening phase to peak value at different temperature

Temperature (°C)	12.5	15	20	25	31
Time (Days)	6	4	3.2	1.5	1.5

Dit-u-dompo (1999) studied the mathematical modeling to predict heat generation during banana (Kluai Hom Thong) respiration. Heat generated from the respiration processes was determined at various temperatures and storage gas compositions (O_2 and CO_2). It was essential to know the amount of heat generated

during respiration process of the stored fruit in order to design and optimization an energy-save refrigeration system for stored fruit. In the experiment, heats of respiration and respiration rate of bananas which stored at 13, 17, 20, and 30 °C in ambient air and CAs containing 4% O_2 - 5% CO_2 and 4% O_2 - 10% CO_2 were calculated. The result showed that the obtained model described the rate of heat produced by the respiration processes of banana and the respiration rate as functions of the storage temperature and O_2 and CO_2 concentrations as shown Figure 2.3, 2.4 and 2.5 respectively. The results showed that the heat of respiration and respiration rate increased as the storage temperature increased. At a given storage temperature, the heat of respiration of bananas stored in ambient air was higher than that stored in CAs containing 4% O_2 - 5% CO_2 and 4% O_2 - 10% CO_2, respectively. Moreover, the models were used in calculating the rates of heat produced by bananas stored under a controlled atmosphere (CA) condition at various storage temperatures. The results showed good agreements between the predicted and observed values. Therefore, the models could be used for determining the rate of heat released from bananas stored in a CA storage room.

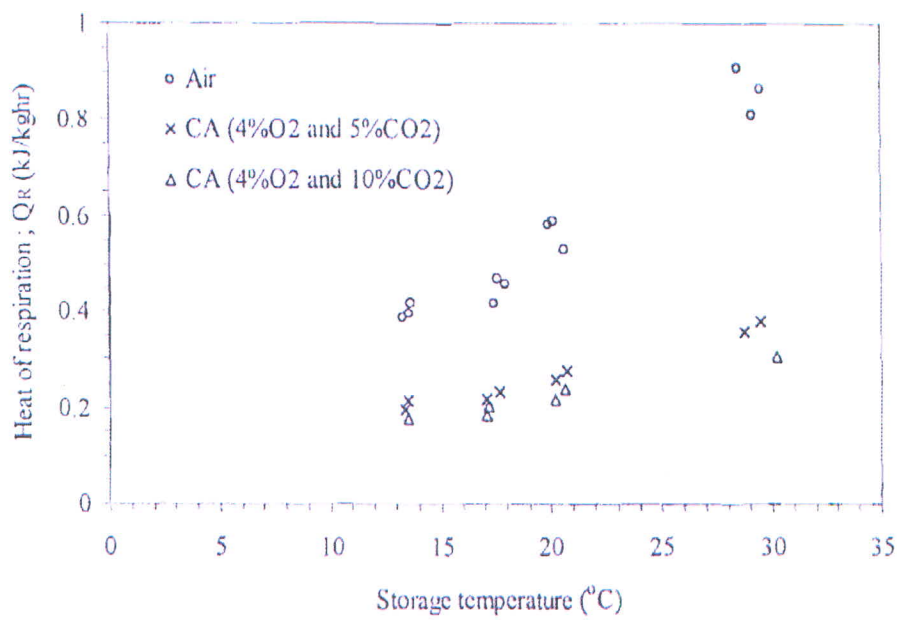

Figure 2.3 Heats of respiration of bananas which stored at 13, 17, 20 and 30 °C in ambient air and CAs containing 4% O_2 - 5% CO_2 and 4% O_2 - 10% CO_2.

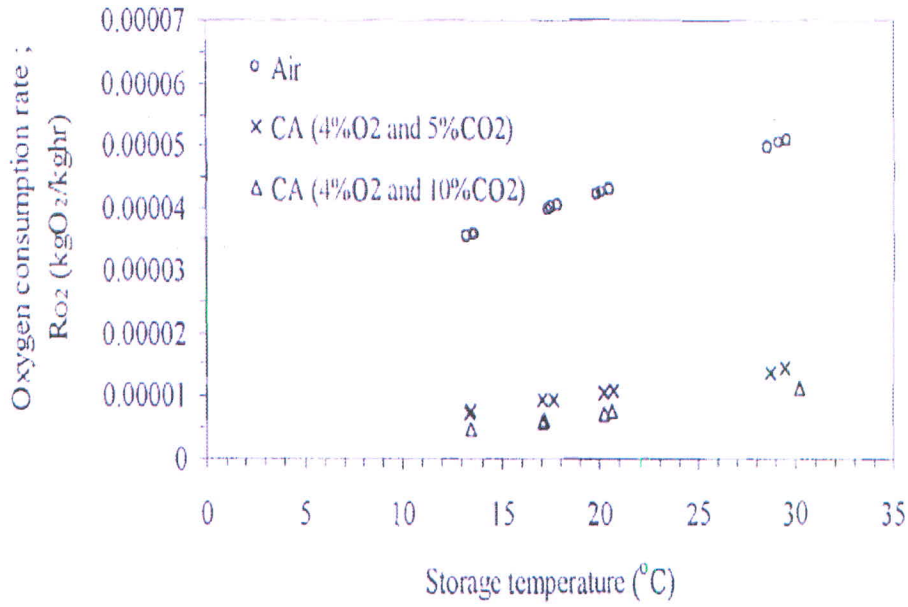

Figure 2.4 O_2 consumption rate of bananas which stored at 13, 17, 20 and 30 °C in ambient air and CAs containing 4% O_2 - 5% CO_2 and 4% O_2 - 10% CO_2.

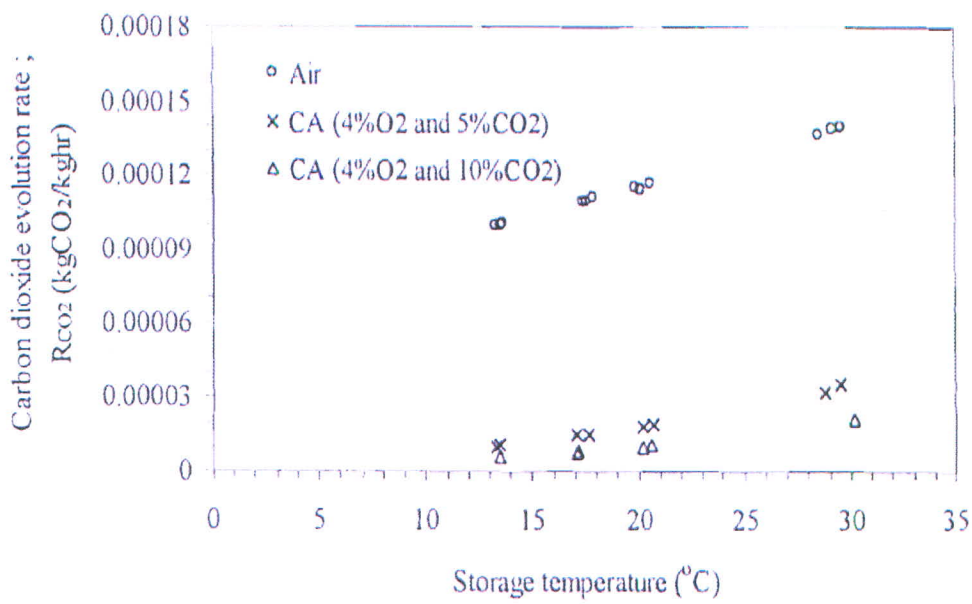

Figure 2.5 CO_2 evolution rate of bananas which stored at 13, 17, 20 and 30 °C in ambient air and CAs containing 4% O_2 - 5% CO_2 and 4% O_2 - 10% CO_2.

Jirapattarasakul (2002) studied heat treatment and respiration model of Mango (Nam Dok Mai). The result showed that respiration kinetic parameters of mango after heat treatments tended to decrease with the increases of heat treatment temperature and the duration time as shown in Figure 2.6. Thus, heat treatment at suitable temperature and duration time could play a role in decreasing respiration rate of mango after heat treatment. The effect of heat treatments on fruit qualities was found that heat treatments at 42°C for 85 min and 46°C for 75 minutes could also reduce weight loss percentage, retard the fruit softening, and increase the color development of mango during storage under MAP at 13°C. Besides, combination between heat treatment and MAP could prolong storage life to 45 days which is 10 days longer than that of fruit without heat treatments. Therefore, appropriate heat treatment could extend the storage time of mango kept under MAP condition.

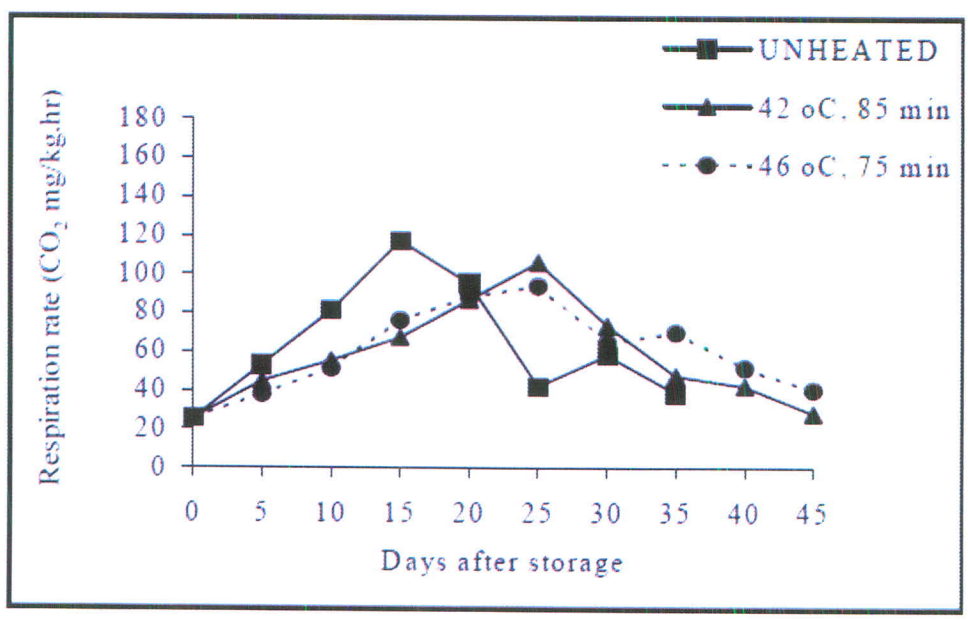

Figure 2.6 Respiration rate of unheated mango, heat treatment at 42 and 46°C for 85 and 75 min, respectively stored at 13°C.

2.4 pH Indicator

The pH indicator is the halochromic chemical compound or the compound which changes color when pH changes occur. The pH indicator can be added in small amounts to a solution so that the pH (acidity or basicity) of the solution can be determined visually. The general reaction scheme of a pH indicator can be formulated as follow equation.

$$HIn + H_2O \rightleftharpoons H_3O^+ + In^- \qquad (2)$$

2.4.1 Bromothymol Blue

Bromothymol blue is a chemical indicator for weak acids and bases which is yellow at pH below 6.0 and blue at pH above 7.6. The pKa for bromothymol blue is 7.10. The chemical is also used for observing photosynthetic activities or respiratory indicators. It will turns from blue to yellow when CO_2 is added. The mechanism of bromothymol blue in acid and basis form is shown in Figure 2.7.

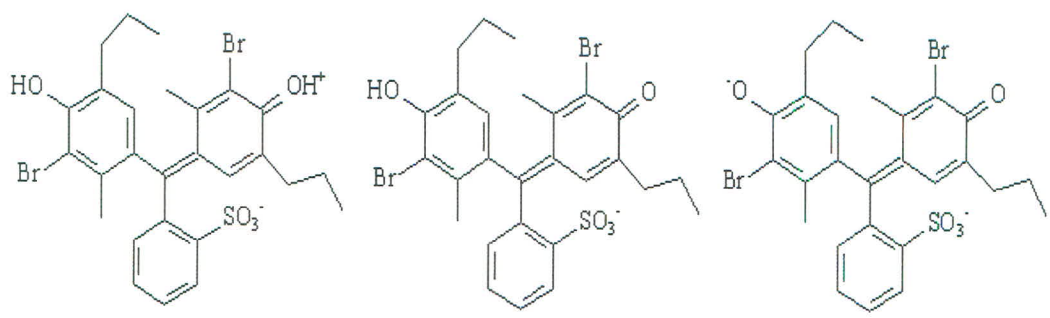

Figure 2.7 Mechanism of bromoyhymol blue indicator in yellow color (left), intermediate between yellow and blue (middle) and blue color (right).

2.5 Structure of Layer Silicate

In the synthesis of nanocomposites, layer silicates are natural or synthetic minerals. They consist of very thin layers that are usually bound together with counter-ions. Their basic building blocks are tetrahedral sheets and octahedral sheets. Tetrahedral sheets compose of silicon which surrounded by four oxygen atoms and octahedral sheets compose of a metal like aluminum which surrounded by six oxygen atoms. Therefore, tetrahedral sheet is fused with an octahedral sheet in 1:1 layered structures (e.g. in kaolinite), whereby the oxygen atoms are shared. On the other hand, the crystal lattice of 2:1 layered silicates or 2:1 phyllosilicates (e.g. in montmorillonite, hectorite and saponite) consists of two-dimensional layers where a central octahedral sheet of alumina is fused to two external silica tetrahedral by the tip, so that the oxygen ions of the octahedral sheet also belong to the tetrahedral sheets, as shown in Figure 2.8. The layer thickness is around 1 nm and the lateral dimensions may vary from 300A° to several microns depending on the particulate silicate (Pavlidou S. and Papaspyrides C., 2008). These layers stack with a regular electrostatic force in between them called the interlayer or the gallery. Isomorphic substitution within the layer (for example, Al^{3+} replaced by Mg^{2+} or by Fe^{2+} in montmorillonite, or Mg^{2+} replaced by Li^{+} in hectorite) generates negative charges. The imbalance of the surface negative charges is compensated by exchangeable cations (typically Na^{+} and Ca^{2+}). The parallel layers are linked together by weak electrostatic forces. As the forces that hold the layer together are relatively weak, the intercalation between the layers is easy. These layers stack with a regular electrostatic force in between them called the interlayer or the gallery. Isomorphic substitution within the layer (for example, Al^{3+} replaced by Mg^{2+} or by Fe^{2+} in montmorillonite, or Mg^{2+} replaced by Li^{+} in hectorite) generates negative charges. The imbalance of the surface negative charges is compensated by exchangeable cations (typically Na^{+} and Ca^{2+}). The parallel layers are linked together by weak electrostatic forces. As the forces that hold the layer together are relatively weak, the intercalation between the layers is easy.

This type of clay is characterized by a moderate negative surface charge (known as the cation exchange capacity, CEC and expressd in mequiv/100g) which

is an important factor to define the equilibrium layer spacing. The charge of the layer is not locally constant as it varies from layer to layer and must rather be considered as an average value over the whole crystal. When the hydrated cations are ion-exchanged with organic cations such as more bulky alkylammoniums, it usually results in a larger interlayer spacing (Pavlidou, 2008).

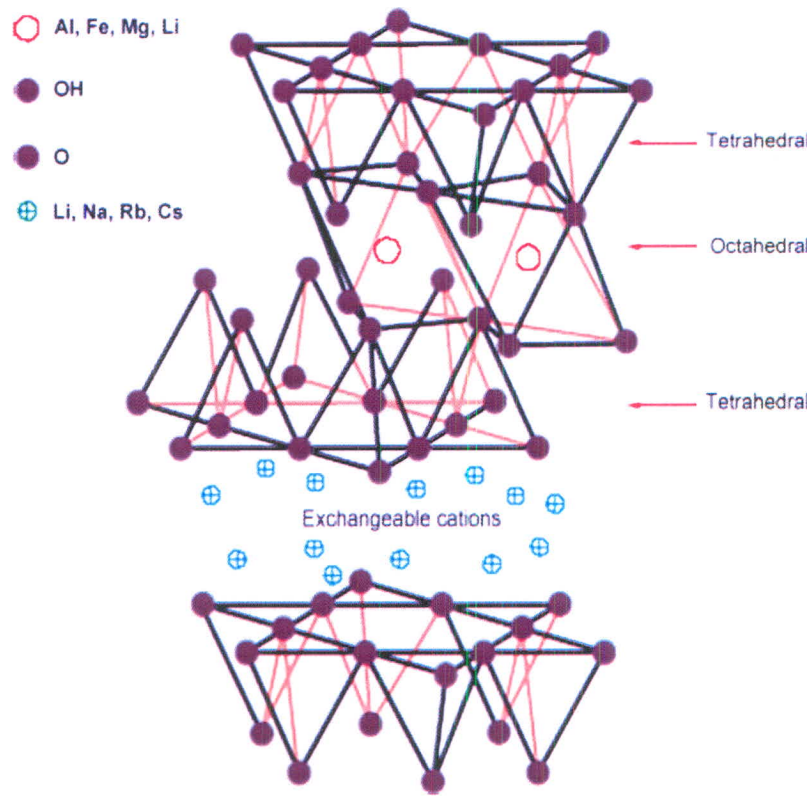

Figure 2.8 Structure of 2:1 layer silicate (Pavlidou, 2008).

2.6 Porous Clay Heterostructure (PCH)

Porous clay heterostructure (PCH) is a porous material that has been developed due to the special properties i.e. improves the ability of adsorption by high surface area. PCH can be prepared by using surfactant incorporated within the galleries of clay. Cationic surfactants will intercalate between the sheets of clay. Then PCH is synthesized by polymerization of the silica source such as

tetraethoxysilane (TEOS) in the presence of surfactant micelles. However, in the preparation of PCH, calcination at high temperature (600-650°C) or solvent extraction method are necessary to remove the surfactant in order to obtain complete silica structure.

Mattayan *et al.* (2009) prepared porous clay heterostructure (PCH) at various ratios of dodecylamine and TEOS and modified the PCH surface by Fe ions (Fe^{2+} and Fe^{3+}). Subsequently, PCH was blended with polylactide to obtain polylactide-clay nanocomposites for food packaging application. The results showed that PCH had surface area of 418-688 m^2/g depending on the various molar ratios of dodecylamine and TEOS. Moreover, magnetic PCH exhibited the bacteriostatic effect against Escherichia coli and Staphylococcus aureus.

To produce porous clay heterostructure with organic-inorganic hybrid structure, the structure of inorganic frame works is combined with organic group in PCH in order to provide the high adsorption property for gas molecules and high selectivity for organic compound.

Srithammaraj *et al.* (2011) prepared porous clay heterostructure (PCH) by the surfactant directed assembly of mesostructured silica within the two-dimensional galleries of clays. PCH was synthesized by the polymerization of tetraethoxysilane (TEOS) in the presence of surfactant micelles within the galleries of bentonite. Moreover, porous clay was modified with organic group (methyltriethoxysilane and 3-mercaptopropyl triethoxysilane) by co-condensation method with TEOS to produce organic-inorganic hybrid material, HPCH and MPPCH respectively. Then, the synthesized PCH, HPCH and MPPCH were blended with polypropylene (PP) to produce PCH/PP, HPCH/PP and MPPCH/PP for ethylene scavenging blown films. From the surface characterization, surface area of PCH, HPCH and MPPCH increased to 507.7, 500.3 and 488.7 m^2/g compared with bentonite which had surface area of 31 m^2/g. In addition, PCH, HPCH and MPPCH showed higher efficiency in adsorbing ethylene gas than bentonite due to the non-polar property of organic group. The amount of ethylene adsorption is in order: HPCH >MPPCH > PCH > BTN. HPCH showed the highest amount of ethylene adsorption because of the similarity of the methyl group in HPCH and ethylene gas.

Recently, aminopropyltriethoxysilane (APTES) are widely used in many applications of surface-modified silica source in order to enhance the properties for the desired application.

Wu *et al.* (2006) modified the surface of submicrometer silica spheres from TEOS with aminopropyl and phenyl groups through one-step process. The particles modified with aminopropyl groups (APTES particles) showed higher organic dye (brilliant blue FCF or BBF) adsorption compared with pure TEOS particle and the particle modified with phenyl group (PhTES particles). The adsorption capacity of the particles increases greatly after acidification because the protonation of silanol groups and amine groups on the particle surface enhanced electrostatic attractions with BBF anions. The APTES particles showed the highest adsorption due to the hydrophobic attractions and the electrostatic attraction from amino group as shown in Figure 2.9.

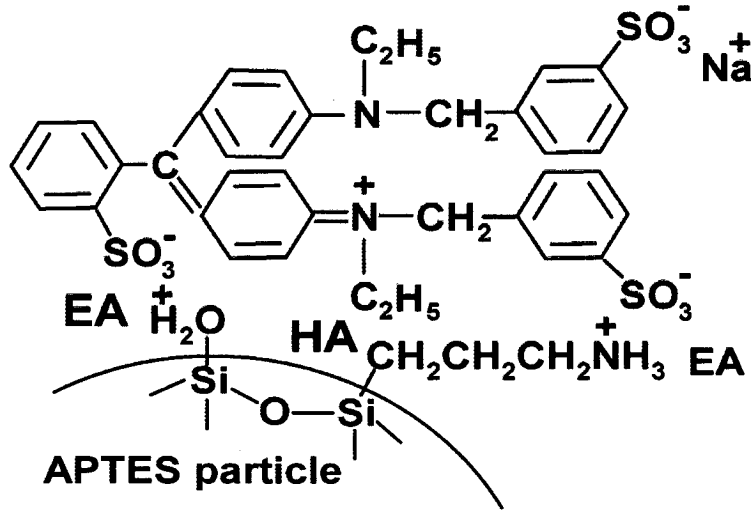

Figure 2.9 Schematic diagrams for the adsorption of BBF by the acidified APTES particles. EA represents electrostatic attraction and HA represents hydrophobic attraction.

Araki *et al.* (2009) synthesized aminopropyl-functionalized mesoporous silica microspheres (AF-MSM) by one-step modified Stober method. The mesoporous silica surface were modified to aminopropyl groups by co-condensation of tetraethoxysilane (TEOS) with 3-aminopropyltriethoxysilane (APTES) at various

mol% of APTES (APTES = 0, 3, 5, 10, 15 and 20 mol %) and dodecylamine (DDA) was used as the catalyst. FT-IR spectra confirmed the presence of aminopropyl groups in AF-MSM by broad band extending from 2800 to 3400 cm^{-1} corresponding to the stretching vibration of NH_3^+ and also by a peak at 1510 cm^{-1} due to the symmetric bending vibration of $-NH_2$. These peaks increased with increasing APTES content. Moreover, AF-MSM was applied to the carbon dioxide adsorbent. Carbon dioxide adsorption capacities increased with increasing with APTES content.

2.7 Clay/Polymer Nanocomposite

Polypropylene (PP) and polyethylene (PE) are the examples of the widely used plastics in large volume because of the advantage such as low cost and wide range of application. To overcome the disadvantage of PP and PE such as low service temperature and to enhance the thermal stability, trying to improve their properties with nanotechnologies was necessary.

Moreover, due to the advantages over other traditional materials such as barrier properties, the use of clay filler in polymer nanocomposite as food packaging materials has increased. In order to improve the barrier properties, clay-polymer nanocomposites are based on a tortuous path around the clay plates, forcing the gas permeation to travel a longer path to diffuse through the film. The increase in path length is a function of the high aspect ratio of the clay filler. Moreover, the resulting from using clay nanoparticles including increased the mechanical properties and thermal properties in polymer.

Clay/polymer nanocomposites are the mixtures of clay in organic polymer. But the homogeneous dispersion of clay in organic polymers is not easy due to the hydrophilicity of clay surface and hydrophobicity of polymer such as polypropylene and polyethylene. Therefore, compatibilizer is important factor to improve the compatibility between polymer and clay.

Surlyn® is one of the compatibilizer which helps to improve the compatibility between polymer and clay by hydrophobic and hydrophilic part respectively. Surlyn® is produced through the copolymerization of ethylene and methacrylic acid.

Methacrylic acid units can be neutralized with a suitable cation commonly Na^{+} or Zn^{+2} as shown in Figure 2.10.

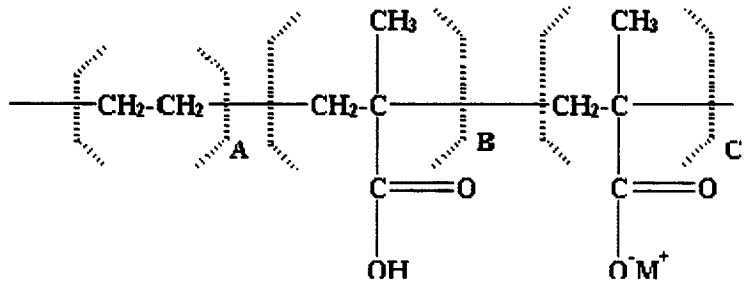

Figure 2.10 Structure of surlyn®.

Tassanawat *et al.* (2007) prepared pH sensitive material used for milk packaging based on polypropylene/organoclay nanocomposites incorporated with indicator dyes using surlyn® as a compatibilizer. The nanoclay composites were fabricated into the sample sheet for color testing and characterizations of thermal and mechanical properties. The results showed that the color of bromothymol blue (BTB) type-film turned from green to yellow whereas bromocresol purple (BP) type-film turn from violet to green correlated with total color difference (TCD) values and titratable acidity (TA) values of fresh milk during storage at ambient temperature. In addition, the clay content had the direct effect on the thermal and mechanical properties of the nanocomposite. The samples with 1 and 3 %wt of organoclay showed the highest Young's modulus, strain at break and toughness but PP/organoclay nanocomposites started to drop in all mechanical properties, except the tensile strength, when the organoclay is incorporated more than 3%wt (5 and 7%wt).

Seephueng *et al.* (2008) prepared colored pH sensor for fish freshenss packaging in order to evaluate the freshness of fresh fish spoilage. The processing of pH-sensitive film based on PP/organomodified clay nanocomposites, using surlyn® as a compatibilizer, laminated with the layer of pH dye. Subsequently, the pH fabricated by using spin-coater and was attached to PP/clay nanocomposite films using a laminating machine (at 160°C). The result showed that the total color difference (TCD) values of bromocresol green (BCG) type indicator correlated with

aerobic plate count (APC) and total volatile basic nitrogen (TVB-N) of fresh fish during spoilage and the color of pH sensor change from yellow to green. Moreover, it was found that incorporation of clay (1, 3 and 5 wt %) increased the thermal stability and gas barrier properties of PP. The clay content had the direct effect on the mechanical properties. Young's modulus, stress at break and % elongation at break is highest at the improvement for sample at 1%wt of organoclay. Conversely, all mechanical properties of PP/clay nanocomposite started to drop when the organoclay is incorporated more than 1%wt resulting from agglomeration and impurity of the organoclay.

Shah *et al.* (2006) prepared blown films of nanocomposites prepared from low density polyethylene and a sodium ionomer of poly(ethylene-co-methacrylic acid). The organoclay content and film blowing conditions were varied to determine the effect of platelet concentration, exfoliation and orientation on film properties. Mechanical properties including stiffness, puncture resistance and resistance to tear propagation were evaluated and compared to corresponding properties of unfilled polymer films. Permeability of the films to moisture and common atmospheric gases like oxygen, nitrogen, and carbon dioxide was also measured using standard testing methods. Films prepared from nanocomposites based on the ionomer exhibited greater improvements in mechanical and barrier properties over unfilled polymer compared to similar films prepared from nanocomposites based on LDPE. This is due to the greater degree of organoclay exfoliation achieved in the ionomer compared to LDPE. The addition of 3 wt% MMT to the ionomer increased the tensile modulus of blown films by an average of 50% without sacrificing much tear strength, puncture resistance or film extensibility. Gas permeability in these films was lowered by 40% and moisture transmission rate was reduced by 60%.

Santamaria *et al.* (2012) studied the structure and mechanical properties of blown films of ionomer compatibilized LDPE nanocomposites. Blown films based on low density polyethylene (LDPE) organoclay nanocomposites (NCs) were obtained by melt extrusion followed by film blowing, using a zinc ionomer of poly(ethylene-co-methacrylic acid) (Pema-Zn) as a compatibilizer. The parameters studied were the compatibilizer and the montmorillonite (MMT) contents that ranged from 0 to 20% and from 0 to 5%, respectively. The presence of clay hindered Pema-

Zn crystallization indicating the existence of interaction between the Pema-Zn and the clay. Analysis of the nanostructure showed that the MMT was found inside microscopic domains of Pema-Zn distributed throughout the LDPE matrix. The addition of Pema-Zn improved the dispersion of the clay in LDPE films resulting in synergistic improvements in the mechanical properties. These improvements occur both in the machine and transverse directions. Thus, the presence of Pema-Zn is a determining factor in biaxiality and can clearly be attributed to the bidimensional laminar structure of clays such as MMT.